Polymer Chemistry

RSC Publishing

PAPER

View Article Online
View Journal | View Issue

Cite this: *Polym. Chem.*, 2013, **4**, 5321

Conjugated random copolymers of benzodithiophene–benzooxadiazole–diketopyrrolopyrrole with full visible light absorption for bulk heterojunction solar cells

Jian-Ming Jiang, Hsiu-Cheng Chen, His-Kuei Lin, Chia-Ming Yu, Shang-Che Lan, Chin-Ming Liu and Kung-Hwa Wei*

We have used Stille coupling polymerization to synthesize a series of new donor–acceptor (D–A) conjugated random copolymers—**PBDTT-BO-DPP**—that comprise electron-rich alkylthienyl-substituted benzodithiophene (**BDTT**) units in conjugation with electron-deficient 2,1,3-benzooxadiazole (**BO**) and diketopyrrolopyrrole (**DPP**) moieties that have complementary light absorption behavior. These polymers exhibited excellent thermal stability with thermal degrading temperatures higher than 340 °C. Each of these copolymers exhibited (i) broad visible light absorption from 400 to 900 nm and (ii) a low optical band gap that is smaller than 1.4 eV and a low-lying highest occupied molecular orbital that is deeper than −5.22 eV. As a result, bulk heterojunction photovoltaic devices derived from these polymers and fullerenes provided a high short-circuit current density that is larger than 12 mA cm^{-2}. In particular, a photovoltaic device prepared from the **PBDTT-BO-DPP** (molar ratio, 1 : 0.5 : 0.5)/$PC_{71}BM$ (w/w, 1 : 2) blend system with 1-chloronaphthalene (1 volume%) as an additive exhibited excellent photovoltaic performance, with a value of V_{oc} of 0.73 V, a high short-circuit current density of 17 mA cm^{-2}, a fill factor of 0.55, and a promising power conversion efficiency of 6.8%, indicating that complementary light-absorption random polymer structures have great potential for increasing the photocurrent in bulk heterojunction photovoltaic devices.

Received 25th January 2013
Accepted 27th February 2013

DOI: 10.1039/c3py00132f

www.rsc.org/polymers

Introduction

Polymer solar cells (PSCs) have attracted considerable attention as promising energy resources because they allow the production of low-cost, light-weight, large-area, flexible devices through ink-jet printing and roll-to-roll solution processing.[1] Tremendous efforts have been made toward improving the power conversion efficiencies (PCEs) of bulk heterojunction (BHJ) devices that incorporate conjugated polymers and fullerene derivatives as their electron-donating and -accepting components, respectively.[2] The PCE of a solar cell device is the product of its short-circuit current density (J_{sc}), open-circuit voltage (V_{oc}), and fill factor (FF). In a device having a BHJ-structured active layer, the open-circuit voltage is typically linearly proportional to the difference in energy between the highest occupied molecular orbital (HOMO) of the polymer and the lowest unoccupied molecular orbital (LUMO) of the fullerene; therefore, the value of V_{oc} can be increased either by elevating the LUMO energy level of the fullerene or by decreasing the HOMO energy level of the polymer.[3] Increases in FFs can occur mainly through improving active layer morphologies for balanced charge transport and carrying out extensive device optimization.[4,5] Whereas, the value of J_{sc} is determined by the amount of absorbed light that results from the band gap of the polymer, the layer thickness and the breadth of the absorption as well as the active layer morphology that dictates the transport of electrons and holes to the cathode and the anode, respectively. Because conjugated polymers typically absorb in only a limited region of the solar spectrum, many PSCs do not exhibit high PCEs. The fabrication of tandem BHJ solar cells and the use of low-band gap polymers blended with fullerenes as the active layer are two main approaches that have been used to enhance the absorption of solar light. Tandem solar cells usually comprise multiple single-BHJ cells stacked in series, with each layer featuring a different absorption band; the resulting combined absorption covers a broader region of the solar spectrum.[6] The fabrication of a tandem solar cell, however, is more complicated than that of a single solar cell because not only proper processing conditions must be tailored to all cells that are in series but also additional interfacial layers between cells are usually required. For single cells, the development of new broadly absorbing conjugated polymers is a necessary approach toward achieving high-efficiency PSCs. The donor–acceptor (D–A) approach, in which a perfectly alternating pattern of covalently bound electron-rich and -poor chemical units comprises the backbone, is frequently adopted

Department of Materials Science and Engineering, National Chiao Tung University, 1001 Ta Hsueh Road, Hsinchu, 30050, Taiwan, ROC. E-mail: khwei@mail.nctu.edu.tw; Fax: +886-3-5724727; Tel: +886-3-5731771

to obtain conjugated polymers exhibiting low band gaps as a result of the internal charge transfer between the D and A units.[7] Although tuning the band gap of a D–A conjugated polymer while maintaining a low-lying HOMO for a high value of V_{oc} can be carried out by adopting a weak electron donor conjugated with a strong electron acceptor, it has limited effect on broadening the absorption of the solar spectrum by the D–A conjugated polymer. One approach toward broadening the absorption of the solar spectrum involves the use of a random D–A conjugated polymer exhibiting complementary light absorption from different D units in conjugation with various A units.[8] For this approach, one architecture is concerned with using two D units for copolymerizing with one A unit.[8a–d] The other architecture involves the copolymerization of two different A units with one D unit to form random polymer structures.[8e–h] The latter polymer architecture will result in consistent values of V_{oc} for the photovoltaic devices because its HOMO and LUMO energy levels are largely localized on the D and A units, respectively, from theoretical studies. These random copolymers exhibit considerably broadened absorptions and/or two distinct absorption peaks in the short and long wavelength regions; accordingly, random D–A polymer structures with complementary light absorption units have great potential for increasing the photocurrent in PSCs.

Among the various low-band gap conjugated polymers, D–A conjugated polymers adopting diketopyrrolopyrrole (**DPP**), which possesses a lactam structure, as a strong electron-acceptor unit have emerged as interesting materials in PSC applications;[9a,b] they possess planar and well-conjugated skeletons that give rise to strong π–π interactions and result in absorptions in the near-infrared (NIR) region, 600–900 nm, as well as high carrier mobility.[9c–e] BHJ PSCs based on conjugated polymers containing **DPP** units have been reported by several research groups to exhibit PCEs of 4–6.5%.[9f–j] On the other hand, benzooxadiazole (**BO**), which adopts a quinoid structure, is also a strongly electron-accepting moiety that has been used in conjugated polymers for PSCs exhibiting PCEs of up to 5–6%,[10,11c] with two strong absorption peaks near 400 and 600 nm, respectively.

Herein, we report the synthesis of new conjugated random copolymers featuring diketopyrrolopyrrole (**DPP**) and benzooxadiazole (**BO**) as electron-acceptor units in conjugation with electron-donating thienyl-substituted benzodithiophene (**BDTT**)[11] units that exhibit full-range absorption of visible light and, thereby, provide high-efficiency BHJ solar cells.

Experimental section

Materials and synthesis

2,6-Bis(trimethyltin)-4,8-bis(5-ethylhexyl-2-thienyl)benzo[1,2-*b*:4,5-*b*′]dithiophene (**M1**),[11] 4,7-bis(5-bromothien-2-yl)-5,6-bis(octyloxy)benzo[*c*][1,2,5]oxadiazole (**M2**),[10] and 3,6-bis(5-bromothien-2-yl)-2,5-bis(2-ethylhexyl)pyrrolo[3,4-*c*]pyrrole-1,4-dione (**M3**)[9a] were prepared according to the reported procedures. [6,6]-Phenyl-C_{61}-butyric acid methyl ester ($PC_{61}BM$) and [6,6]-phenyl-C_{71}-butyric acid methyl ester ($PC_{71}BM$) were purchased from Nano-C. All other reagents were used as received without further purification, unless stated otherwise.

General procedure for the synthesis of PBDTT-BO-DPP through Stille coupling

Alternating polymer PBDTT-BO-DPP (1 : 0.3 : 0.7), P1. A solution of **M1** (100 mg, 0.11 mmol), **M2** (23.1 mg, 0.033 mmol), **M3** (52.7 mg, 0.077 mmol), and tri(*o*-tolyl)phosphine (2.6 mg, 8.0 mol%) in dry chlorobenzene (4 mL) was degassed for 15 min. Tris(dibenzylideneacetone)dipalladium (2.0 mg, 2.0 mol%) was added under N_2 and then the reaction mixture was heated at 130 °C for 48 h. After cooling to room temperature, the solution was added dropwise into MeOH (100 mL). The crude polymer was collected, dissolved in $CHCl_3$, and reprecipitated in MeOH. The solid was washed with MeOH, acetone, and $CHCl_3$ in a Soxhlet apparatus. The $CHCl_3$ solution was concentrated and then added dropwise into MeOH. The solids were collected and dried under vacuum to give **PBDTT-BO-DPP** (1 : 0.3 : 0.7), **P1** (140 mg, 80%). Anal. calcd: C, 69.70; H, 7.14; N, 2.41. Found: C, 67.85; H, 7.02; N, 2.53%.

Alternating polymer PBDTT-BO-DPP (1 : 0.5 : 0.5), P2. Using a procedure similar to that described above for **P1**, a mixture of **M1** (100 mg, 0.11 mmol), **M2** (38.4 mg, 0.055 mmol), and **M3** (37.5 mg, 0.055 mmol) in dry chlorobenzene (4 mL) was polymerized to give **P2** (120 mg, 70%). Anal. calcd: C, 69.33; H, 7.18; N, 2.53. Found: C, 67.98; H, 7.57; N, 2.97%.

Alternating polymer PBDTT-BO-DPP (1 : 0.7 : 0.3), P3. Using a procedure similar to that described above for **P1**, a mixture of **M1** (100 mg, 143 mmol), **M2** (53.7 mg, 0.077 mmol), and **M3** (22.5 mg, 0.033 mmol) in dry chlorobenzene (4 mL) was polymerized to give **P3** (122 mg, 70%). Anal. calcd: C, 69.18; H, 7.09; N, 2.52. Found: C, 68.01; H, 7.39; N, 2.85%.

Measurements and Characterization

^{1}H NMR spectra were recorded using a Varian UNITY 300-MHz spectrometer. Thermogravimetric analysis (TGA) was performed using a TA Instruments Q500; the thermal stabilities of the samples were determined under N_2 by measuring their weight losses while heating at a rate of 20 °C min^{-1}. Size exclusion chromatography (SEC) was performed using a Waters chromatography unit interfaced with a Waters 1515 differential refractometer; polystyrene was the standard; the temperature of the system was set at 45 °C and $CHCl_3$ was the eluent. UV-Vis spectra of dilute dichlorobenzene (DCB) solutions (1×10^{-5} M) were recorded at approximately 25 °C using a Hitachi U-4100 spectrophotometer. Solid films for UV-Vis analysis were obtained by spin-coating polymer solutions onto quartz substrates. Cyclic voltammetry (CV) of the polymer films was performed using a BAS 100 electrochemical analyzer operated at a scan rate of 50 mV s^{-1}; the solvent was anhydrous MeCN containing 0.1 M tetrabutylammonium hexafluorophosphate ($TBAPF_6$) as the supporting electrolyte. The potentials were measured against a Ag/Ag^+ (0.01 M $AgNO_3$) reference electrode; ferrocene/ferrocenium ion (Fc/Fc^+) was used as the internal standard (0.09 V). The onset potentials were determined from the intersection of two tangents drawn at the rising and

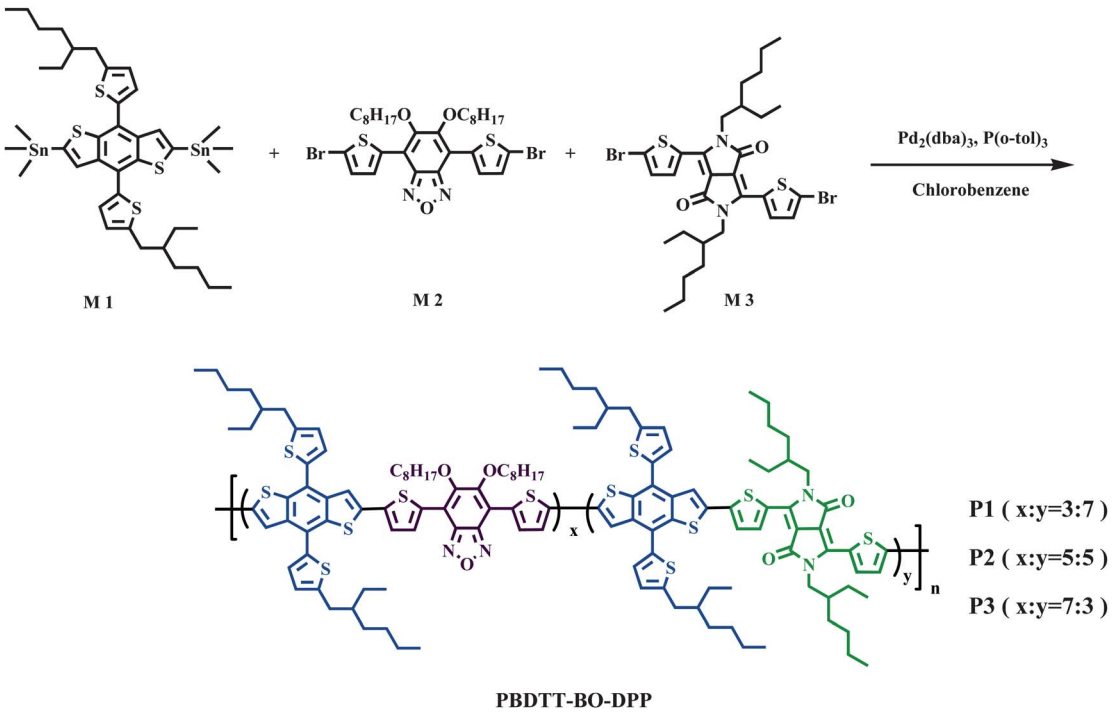

Scheme 1 Synthesis of the copolymers **P1**, **P2**, and **P3**.

Table 1 Molecular weights and thermal properties of the polymer

Polymer	M_w[a]	M_n[a]	PDI[a]	T_d[b]
P1	75.1k	20.3k	3.7	408
P2	87.7k	35.1k	2.5	357
P3	101.5k	37.6k	2.7	345
PBDTTBO	145.8k	52.1k	2.8	333
PBDTTDPP	57.3k	18.5k	3.1	452

[a] Values of M_n, M_w, and PDI of the polymers were determined through GPC (in $CHCl_3$ using polystyrene standards). [b] The 5% weight-loss temperatures (°C) in the air.

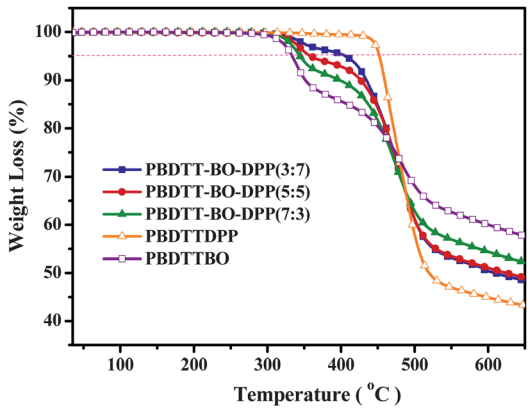

Fig. 1 TGA thermograms of the copolymers **P1**, **P2**, and **P3**, recorded at a heating rate of 20 °C min^{-1} under a N_2 atmosphere.

background currents of the cyclic voltammogram. HOMO and LUMO energy levels were estimated relative to the energy level of the ferrocene reference (4.8 eV below vacuum level). Topographic and phase images of the polymer:fullerene films (surface area: 5 × 5 μm^2) were recorded using a Digital Nanoscope III atomic force microscope operated in the tapping mode under ambient conditions. The thicknesses of the active layers in the devices were measured using a VeecoDektak 150 surface profiler.

Fabrication and Characterization of Photovoltaic Devices

Indium tin oxide (ITO)-coated glass substrates were cleaned stepwise in detergent, water, acetone, and isopropyl alcohol (ultrasonication; 20 min each) and then dried in an oven for 1 h; subsequently, the substrates were treated with UV ozone for 30 min prior to use. A thin layer (*ca.* 20 nm) of polyethylenedioxythiophene:polystyrenesulfonate (PEDOT:PSS, Baytron P VP AI 4083) was spin-coated (5000 rpm) onto the ITO substrates. After baking at 140 °C for 20 min in air, the substrates were transferred to a N_2-filled glove box. The polymer and PCBM were co-dissolved in DCB at various weight ratios, but with a fixed total concentration (40 mg mL^{-1}). The blend solution was stirred continuously for 12 h at 90 °C and then filtered through a PTFE filter (0.2 μm); the photoactive layer was obtained by spin coating the blend solution onto the ITO/PEDOT:PSS surface at a rate between 600 and 2500 rpm for 60 s. The thicknesses of the photoactive layers were approximately 80–105 nm. The devices were finished for measurement after thermal deposition of a 30 nm film of Ca and then a 100 nm film of Al as the cathode at a pressure of approximately

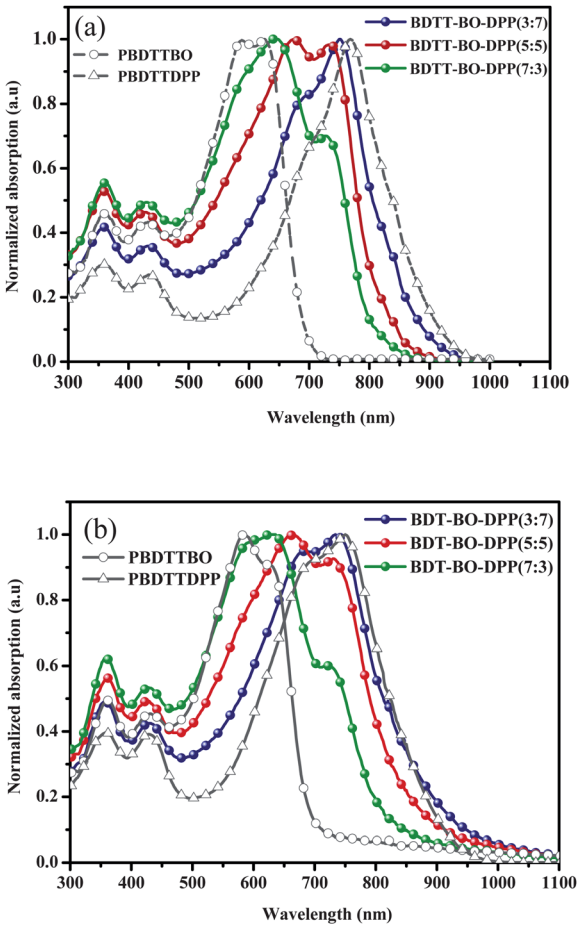

Fig. 2 UV-Vis absorption spectra of the polymers **PBDTTBO**, **PBDTTDPP**, **P1**, **P2**, and **P3** as (a) dilute solutions (1×10^{-5} M) in DCB and (b) solid films.

Table 2 Optical properties of the polymers

	$\lambda_{max,abs}$ (nm)		FWHM (nm)		λ_{onset} (nm)	
	Solution	Film	Solution	Film	Film	E_g^{opt} (eV)
P1	752	680, 740	184	232	950	1.31
P2	677, 736	664, 737	236	264	920	1.34
P3	640, 722	630, 722	244	258	845	1.46
PBDTTBO	590, 620	590, 630	150	160	695	1.78
PBDTTDPP	764	750	170	212	950	1.31

1×10^{-6} mbar. The effective layer area of one cell was 0.1 cm^2. The current density–voltage (*J–V*) characteristics were measured using a Keithley 2400 source-meter. The photocurrent was measured under simulated AM 1.5 G illumination at 100 mW cm^{-2} using a Xe lamp-based Newport 66902 150-W solar simulator. A calibrated silicon photodiode with a KG-5 filter was employed to check the illumination intensity. External quantum efficiencies (EQEs) were measured using an SRF50 system (Optosolar, Germany). A calibrated mono-silicon diode exhibiting a response at 300–1000 nm was used as a reference. For hole mobility measurements, hole-only devices were fabricated having the structure ITO/PEDOT:PSS/polymer:PCBM/Au. The hole mobility was determined by fitting the dark *J–V* curve to the space-charge-limited current (SCLC) model.[12]

Results and discussion

Synthesis and characterization of the polymers

Scheme 1 outlines the general synthetic strategy that we used to obtain the random polymers. To ensure good solubility of the **BO** derivative **M2**, we positioned two octyloxy chains on the **BO** ring. We synthesized **M1**, **M2**, and **M3** using the reported methods.[9a,10,11] After Stille coupling using Pd_2dba_3 as the catalyst in chlorobenzene at 130 °C for 48 h, we obtained the polymers **P1**, **P2**, and **P3** in yields of 70–80%. We determined the solubilities of these copolymers in various solvents at a concentration of 5 mg mL^{-1}. **PBDTTBO**, **P2**, and **P3** were completely soluble in $CHCl_3$, chlorobenzene, and DCB at room temperature, whereas **P1** and **PBDTTDPP** were soluble only after heating at 50 °C. We determined the weight-average molecular weights (M_w) of these polymers (Table 1) through gel permeation chromatography (GPC), against polystyrene standards, with $CHCl_3$ as the eluent.

Thermal stability

We used TGA to determine the thermal stabilities of the polymers (Fig. 1). In air, the 5% weight-loss temperatures (T_d) of **P1**,

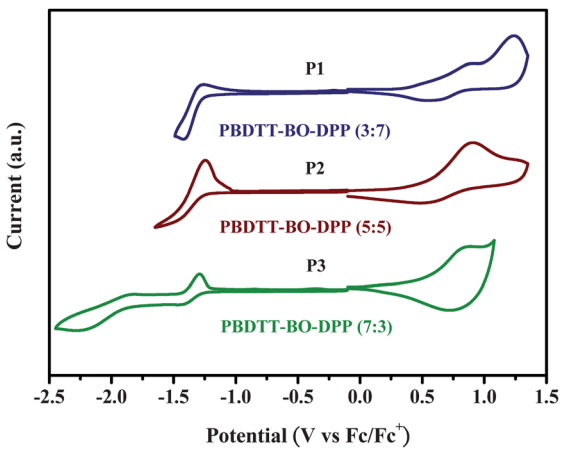

Fig. 3 Cyclic voltammograms of solid films of the copolymers **P1**, **P2**, and **P3**.

Table 3 Electrochemical properties of the copolymers **P1**, **P2**, and **P3**

	E_{onset}^{ox} [a] (V)	E_{onset}^{red} [a] (V)	HOMO[b] (eV)	LUMO[b] (eV)	E_g^{opt} (eV)
P1	0.42	−1.27	−5.22	−3.53	1.69
P2	0.52	−1.26	−5.32	−3.54	1.78
P3	0.56	−1.27	−5.36	−3.53	1.83

[a] The potentials were measured against a Ag/Ag^+ (0.01 M $AgNO_3$) reference electrode; ferrocene/ferrocenium ion (Fc/Fc^+) was used as the internal standard (0.09 V). [b] HOMO and LUMO energy levels determined using the equations HOMO = $(-4.8 + E^{ox})$ eV and LUMO = $(-4.8 + E^{red})$ eV.

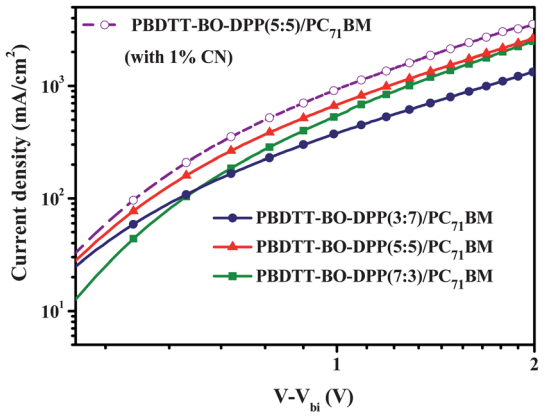

Fig. 4 Dark *J–V* curves for the hole-dominated carrier devices incorporating the polymers blend with $PC_{71}BM$ [blend ratio, 1 : 2 (w/w)], and the **P2**/$PC_{71}BM$ blend prepared in the presence of CN (1 vol%).

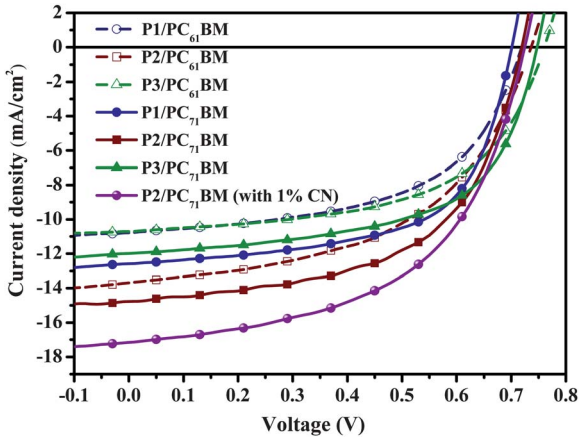

Fig. 5 *J–V* characteristics of PSCs incorporating copolymer:$PC_{61}BM$ blends, copolymer:$PC_{71}BM$ blends, and the **P2**:$PC_{71}BM$ blend prepared in the presence of CN (1 vol%); each blend ratio, 1 : 2 (w/w).

P2, and **P3** were 408, 357, and 345 °C, respectively. Thus, they all exhibited good thermal stability—an important characteristic for device fabrication and application.

Optical properties

Fig. 2a and b display the absorption spectra of **PBDTTBO**, **PBDTTDPP**, and **P1–3** in solution (DCB) and in the solid state, respectively; Table 2 summarizes the optical data, including the absorption peak wavelengths ($\lambda_{max,abs}$), absorption edge wavelengths ($\lambda_{edge,abs}$), full widths at half maximum (FWHMs), and optical band gaps (E_g^{opt}). The absorption peaks of **PBDTTBO** and **PBDTTDPP** were located at 590 and 760 nm, respectively, whereas the films of the copolymers **P1–3** exhibited double absorption peaks in the range 300–1000 nm. The relative position and intensity of the absorption peaks of the copolymers **P1–3** were effectively tuned by their composition; for example, the main absorption peaks for the **PBDTT-BO-DPP** copolymers having compositions of 1 : 0.3 : 0.7, 1 : 0.5 : 0.5, and 1 : 0.7 : 0.3 were 680/740, 642/737, and 612/721 nm, respectively; that is, they shifted to a shorter wavelength upon increasing the content of **BO** units. The absorption spectra of the films of each of the copolymers **P1–3** featured two absorption bands: one at 300–500 nm, which we assigned to localized π–π* transitions, and the other, broader band in the long wavelength region, from 500 to 950 nm, corresponding to the intramolecular charge transfer (ICT) between the acceptor **BO** or **DPP** units and the donor **BDTT** units. The absorption spectra of the three polymers in the solid state were similar to their corresponding solution spectra, with slight red-shifts (*ca.* 10–40 nm) of their absorption onsets, indicating that some intermolecular interactions existed in the solid state. The absorption peak near 600 nm underwent a relative red-shift to 750 nm upon increasing the content of **DPP** units; the absorption spectra of the polymers were readily tuned by varying the molar ratio of **BO** units and **DPP** units. The FWHMs of these random **PBDTT-BO-DPP** copolymers having compositions of 1 : 0.3 : 0.7, 1 : 0.5 : 0.5, and 1 : 0.7 : 0.3 were 232, 264, and 258 nm, respectively, approximately 60–100 nm broader than those of **PBDTTBO** and **PBDTTDPP**, implying that the random copolymers would absorb more of the solar spectrum.

The absorption edges for **P1–3** (Table 2) correspond to optical band gaps (E_g^{opt}) of 1.31, 1.34 and 1.46 eV, respectively.

Table 4 Photovoltaic properties of PSCs incorporating **PBDTT-BO-DPP** copolymers

Polymer/$PC_{61}BM$ (w/w; 1 : 2)	V_{oc} (V)	J_{sc} (mA cm^{-2})	FF (%)	PCE (%)	Thickness (nm)
P1	0.72	10.8	55	4.3	82
P2	0.74	13.8	50	5.2	95
P3	0.76	10.7	56	4.6	89

Polymer/$PC_{71}BM$ (w/w; 1 : 2)	V_{oc} (V)	J_{sc} (mA cm^{-2})	FF (%)	PCE (%)	Thickness (nm)	Mobility (cm^2 V^{-1} s^{-1})
P1	0.70	12.5	62	5.5	85	2.3×10^{-3}
P2	0.72	14.7	56	6.0	88	3.3×10^{-3}
P3	0.75	12	59	5.3	93	3.0×10^{-3}
P2/$PC_{71}BM$ (w/w; 1 : 2) (CN, vol%)						
P2(0.5)	0.72	15.2	57	6.2	93	
P2(1.0)	0.73	17	55	6.8	91	5.1×10^{-3}
P2(1.5)	0.73	15.8	56	6.3	89	

Electrochemical properties

We used CV to examine the electrochemical properties, including HOMO and LUMO energy levels, of the random BDTT-based copolymers. Fig. 3 displays the electrochemical properties of the polymers as solid films; Table 3 summarizes the relevant data. Partially reversible n-doping/de-doping processes occurred for these random polymers in the negative potential range; in addition, reversible p-doping/de-doping processes occurred in the positive potential range. The onset oxidation potentials (E^{ox}_{onset}, *vs.* Ag/Ag^{+}) for the copolymers **P1–3** were 0.42, 0.52, and 0.56 V, respectively; in the reductive potential region, the onset reduction potentials (E^{red}_{onset}) were −1.27, −1.26, and −1.27 V, respectively. On the basis of these onset potentials, we estimated the HOMO and LUMO energy levels according to the energy level of the ferrocene reference (4.8 eV below the vacuum level).[13] The HOMO energy levels of the **PBDTT-BO-DPP** copolymers with compositions of 1 : 0.3 : 0.7, 1 : 0.5 : 0.5, and 1 : 0.7 : 0.3 were −5.22, −5.32, and −5.36 eV, respectively, implying that they varied with respect to the modulated ICT strengths resulting from the presence of electron-acceptor units with various electron-withdrawing abilities.[14] The LUMO energy levels of the copolymers **P1–3** were all located within a reasonable range (from −3.53 to −3.54 eV, Fig. 4) and were significantly greater than that of PCBM (*ca.* 4.1 eV); thus, we would expect efficient charge transfer/dissociation to occur in their corresponding devices.[15] In addition, the electrochemical band gaps (E^{ec}_{g}) of the copolymers **P1–3**, estimated from the differences between the onset potentials for oxidation and reduction, were in the range 1.69–1.83 eV; that is, they were slightly larger than the corresponding optical band gaps. This discrepancy between the electrochemical and optical band gaps presumably resulted from the exciton binding energies of the polymers and/or the interface barriers for charge injection.[16]

Hole mobility

Fig. 4 displays the hole mobilities of the devices incorporating the polymer/$PC_{71}BM$ blends at a blend ratio of 1 : 2 (w/w). The hole mobilities of the copolymers **P1–3** blend with $PC_{71}BM$ were 2.3×10^{-3}, 3.3×10^{-3}, and 3.0×10^{-3} $cm^2\ V^{-1}\ s^{-1}$, respectively. When we added a small amount of 1-chloronaphthalene (CN; 1%, by volume relative to DCB) to optimize the miscibility of the **PBDTT-BO-DPP** (1 : 0.5 : 0.5)/$PC_{71}BM$ blend, the hole mobility increased to 5.1×10^{-3} $cm^2\ V^{-1}\ s^{-1}$.

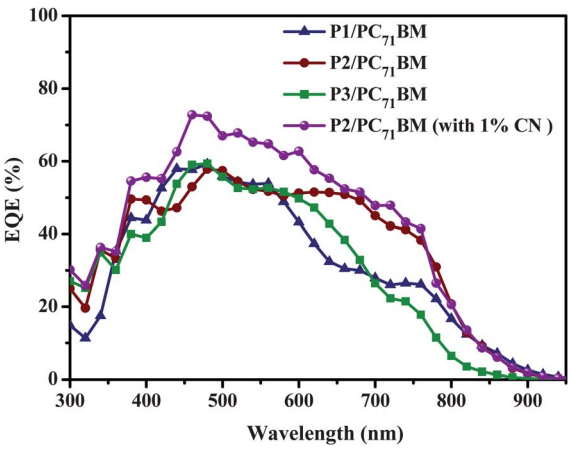

Fig. 6 EQE curves of PSCs incorporating copolymer:$PC_{71}BM$ blends and the **P2**:$PC_{71}BM$ blend prepared in the presence of CN (1 vol%); each blend ratio, 1 : 2 (w/w).

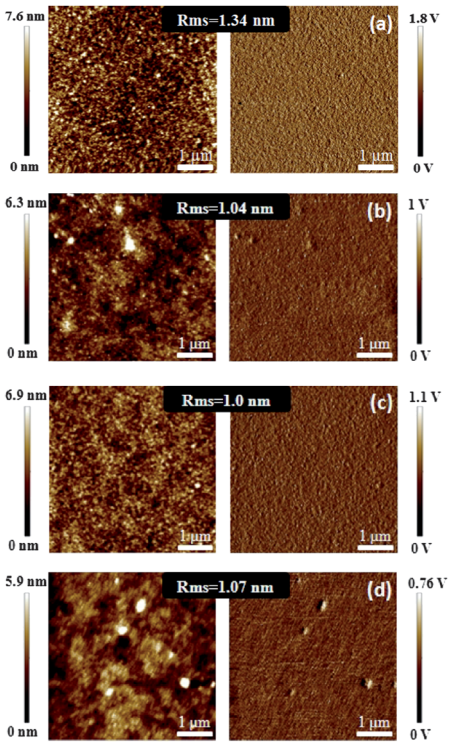

Fig. 7 Topographic AFM images of copolymer:$PC_{71}BM$ (1 : 2, w/w) blends incorporating (a) **P1**, (b) **P2**, (c) **P3**, and (d) **P2** processed in the presence of CN (1 vol%).

Photovoltaic properties

Next, we investigated the photovoltaic properties of the polymers in BHJ solar cells having the sandwich structure ITO/PEDOT:PSS/polymer:fullerene (1 : 2, w/w)/Ca/Al, with the photoactive layers having been spin-coated from DCB solutions of the polymer and fullerene. The optimized weight ratio for the polymer and fullerene was 1 : 2. In this case, we added a small amount of CN (0.5–1.5%, by volume relative to DCB) to optimize the miscibility of the blends. Fig. 5 presents the *J–V* curves of these PSCs; Table 4 summarizes the data. The devices prepared from polymer:$PC_{61}BM$ blends of the copolymers **P1–3** exhibited open-circuit voltages (V_{oc}) of 0.72, 0.74, and 0.76 V, respectively; these values correspond to the difference between the HOMO energy level of the polymer and the LUMO energy level of $PC_{61}BM$ quite well.[17] We suspect that the **PBDTT-BO-DPP** (1 : 0.3 : 0.7) device provided the lowest value of V_{oc} because of its relatively higher-lying HOMO energy level. The J_{sc} of the devices incorporating the copolymers **P1–3** were 10.8, 13.8, and 10.7 mA cm^{-2}, respectively. The devices prepared from polymer:$PC_{71}BM$ blends of the copolymers **P1–3** exhibited V_{oc} of 0.70, 0.72, and 0.75 V, respectively; their J_{sc} were 12.5, 14.7, and

12 mA cm^{-2}, respectively, providing a PCE of 6.0% for the device incorporating **PBDTT-BO-DPP** (1 : 0.5 : 0.5).

Furthermore, we have used a CN additive with different volume ratios in the solution, from 0.5% to 1.5% to process the **PBDTT-BO-DPP** (1 : 0.5 : 0.5)/$PC_{71}BM$ active layer for the devices. When the active layer was processed with 1 vol% CN, the device incorporating the **PBDTT-BO-DPP** (1 : 0.5 : 0.5)/$PC_{71}BM$ (1 : 2, w/w) active layer exhibited the highest value of J_{sc} that represents an increase of 15% over that in the case without the CN additive (17 *vs.* 14.7 mA cm^{-2}), resulting in an optimal PCE of 6.8% (see Table 4). Fig. 6 displays EQE curves of the devices incorporating the polymer:$PC_{71}BM$ blends at a weight ratio of 1 : 2. These devices exhibited significantly broad EQE responses that extended from 300 to 950 nm. We attribute these EQE responses in the visible region to the corresponding absorbances of the active layers, resulting from both the intrinsic absorptions of the polymers and the presence of $PC_{71}BM$, which also absorbs significantly at 300–500 nm. The device based on the blend of **PBDTT-BO-DPP** (1 : 0.5 : 0.5) and $PC_{71}BM$ exhibited the highest EQE response among all of our studied systems, with a maximum value of 72% at 450 nm, consistent with its higher photocurrent. The calculated short-circuit current densities obtained from integrating the EQE curves of the devices incorporating the copolymer blends of **P1–3** with $PC_{71}BM$, and that of **P2** processed with CN (1 vol%) as the additive, were 12.1, 14.1, 11.6, and 16.5 mA cm^{-2}, values that agree reasonably with the measured data (AM 1.5G; discrepancy: <5%).

Moreover, when exploring the decisive factors affecting the efficiencies of PSCs, we must consider not only the absorptions and energy levels of the polymers but also the surface morphologies of the polymer blends.[18] Fig. 7 displays the surface morphologies of our systems, determined using AFM. We prepared samples of the polymer/fullerene blends using procedures identical to those employed to fabricate the active layers of the devices. In each case, we observed quite smooth surfaces for the fullerene blends of the copolymers **P1–3**, with root-mean-square (rms) roughnesses ranging from 1.0 to 1.34 nm. The greater phase segregation and rougher surfaces of the **PBDTT-BO-DPP** (1 : 0.3 : 0.7) blends presumably arose because of poor miscibility with the fullerenes.

Conclusions

We have used Stille copolymerization to prepare a series of new conjugated random copolymers **PBDTT-BO-DPP** that absorb the full spectrum of visible light; they feature random alternating **BDTT** units in conjugation with electron-deficient **BO** and **DPP** moieties, which have complementary light absorption behavior. These polymers possess excellent thermal stability, low-lying HOMO energy levels, and broad absorption bands that extend from the visible to the NIR—desirable properties that make these polymers promising materials for solar cell applications. A device incorporating **PBDTT-BO-DPP** (1 : 0.5 : 0.5) and $PC_{71}BM$ (blend weight ratio, 1 : 2), with CN (1 vol%) as an additive exhibited a high value of J_{sc} of 17 mA cm^{-2} and a PCE of 6.8%, indicating that complementary light-absorption random polymer structures have great potential for increasing the photocurrent in bulk heterojunction photovoltaic devices.

Acknowledgements

We thank the National Science Council, Taiwan, for financial support (NSC 101-3113-P-009-005).

Notes and references

1 (*a*) Y. W. Su, S. C. Lan and K. H. Wei, *Mater. Today*, 2012, **15**, 554; (*b*) X. W. Zhan and D. B. Zhu, *Polym. Chem.*, 2010, **1**, 409; (*c*) M. Helgesen, J. E. Carlé, B. Andreasen, M. Hösel, K. Norrman, R. Sondergaard and F. C. Krebs, *Polym. Chem.*, 2012, **3**, 2649; (*d*) G. Li, R. Zhu and Y. Yang, *Nat. Photonics*, 2012, **6**, 153; (*e*) C. J. Brabec, N. S. Sariciftci and J. C. Hummelen, *Adv. Funct. Mater.*, 2001, **11**, 15; (*f*) F. C. Krebs, *Sol. Energy Mater. Sol. Cells*, 2009, **93**, 394; (*g*) M. M. Wienk, J. M. Koon, W. J. H. Verhees, J. Knol, J. C. Hummelen, P. A. Vanhal and R. A. J. Janssen, *Angew. Chem., Int. Ed.*, 2003, **42**, 3371; (*h*) R. Søndergaard, M. Hösel and F. C. Krebs, *J. Polym. Sci., Part B: Polym. Phys.*, 2013, **51**, 16; (*i*) R. Søndergaard, M. Hösel, D. Angmo, T. L. Olsen and F. C. Krebs, *Mater. Today*, 2012, **15**, 36; (*j*) Y. F. Li, *Acc. Chem. Res.*, 2012, **45**, 723.

2 (*a*) D. Gendron and M. Leclerc, *Energy Environ. Sci.*, 2011, **4**, 1225; (*b*) C. Ottone, P. Berrouard, G. Louarn, S. Beaupré, D. Gendron, M. Zagorska, P. Rannou, A. Najari, S. Sadki, M. Leclerc and A. Pron, *Polym. Chem.*, 2012, **3**, 2355; (*c*) Z. G. Zhang, S. Zhang, J. Ming, C. H. Chui, J. Zhang, M. J. Zhang and Y. F. Li, *Macromolecules*, 2012, **45**, 113; (*d*) T. Y. Chu, J. P. Lu, S. Beaupré, Y. G. Zhang, J. R. Pouliot, S. Wakim, J. Y. Zhou, M. Leclerc, Z. Li, J. F. Ding and Y. Tao, *J. Am. Chem. Soc.*, 2011, **133**, 4250; (*e*) Y. J. He, H. Y. Chen, J. H. Hou and Y. F. Li, *J. Am. Chem. Soc.*, 2010, **132**, 1377; (*f*) Z. He, C. Zhong, X. Huang, W. Y. Wong, H. Wu, L. Chen, S. Su and Y. Cao, *Adv. Mater.*, 2011, **23**, 4636; (*g*) F. Grenier, P. Berrouard, J. R. Pouliot, H. R. Tseng, A. J. Heeger and M. Leclerc, *Polym. Chem.*, 2013, **4**, 1836; (*h*) L. T. Dou, J. B. You, J. Yang, C. C. Chen, Y. J. He, S. Murase, T. Moriarty, K. Emery, G. Li and Y. Yang, *Nat. Photonics*, 2012, **6**, 180; (*i*) J. M. Jiang, M. C. Yuan, K. Dinakaran, A. Hariharan and K. H. Wei, *J. Mater. Chem. A*, 2013, **1**, 4415; (*j*) S. C. Lan, P. A. Yang, M. J. Zhu, C. Y. Yu, J. M. Jiang and K. H. Wei, *Polym. Chem.*, 2013, **4**, 1132.

3 M. Scharber, D. Miihlbacher, M. Koppe, P. Denk, C. Waldauf, A. Heeger and C. Brabec, *Adv. Mater.*, 2006, **18**, 789.

4 M. S. Kim, B. G. Kim and J. Kim, *ACS Appl. Mater. Interfaces*, 2009, **1**, 1264.

5 (*a*) H. Chen, J. Hou, S. Zhang, Y. Liang, G. Yang, Y. Yang, L. Yu, Y. Wu and G. Li, *Nat. Photonics*, 2009, **3**, 649; (*b*) C. Piliego, T. W. Holcombe, J. D. Douglas, C. H. Woo, P. M. Beaujuge and J. M. J. Frechet, *J. Am. Chem. Soc.*, 2010, **132**, 7595; (*c*) G. Zhao, Y. He and Y. Li, *Adv. Mater.*, 2010, **22**, 4355; (*d*) J. M. Jiang, P. A. Yang, T. S. Hsieh and K. H. Wei, *Macromolecules*, 2011, **44**, 9155.

6 J. Y. Kim, K. Lee, N. E. Coates, D. Moses, T. Q. Nguyen, M. Dante and A. J. Heeger, *Science*, 2007, **317**, 222.
7 R. Kroon, M. Lenes, J. Hummelen, P. Blom and B. de Boer, *Polym. Rev.*, 2008, **48**, 531.
8 (*a*) Z. Zhu, D. Waller, R. Gaudiana, M. Morana, D. Mühlbacher, M. Scharber and C. Brabec, *Macromolecules*, 2007, **40**, 1981; (*b*) C. H. Chen, C. H. Hsieh, M. Dubosc, Y. J. Cheng and C. S. Hsu, *Macromolecules*, 2010, **43**, 697; (*c*) Y. He, X. Wang, J. Zhang and Y. Li, *Macromol. Rapid Commun.*, 2009, **30**, 45; (*d*) M. C. Yuan, M. Y. Chiu, C. M. Chiang and K. H. Wei, *Macromolecules*, 2010, **43**, 6270; (*e*) J. Song, C. Zhang, C. Li, W. Li, R. Qin, B. Li, Z. Liu and Z. Bo, *J. Polym. Sci., Part A: Polym. Chem.*, 2010, **48**, 2571; (*f*) B. Burkhart, P. P. Khlyabich, T. C. Canak, T. W. Lajoie and B. C. Thompson, *Macromolecules*, 2011, **44**, 1242; (*g*) B. Burkhart, P. P. Khlyabich and B. C. Thompson, *ACS Macro Lett.*, 2012, **1**, 660; (*h*) C. B. Nielsen, R. S. Ashraf, B. C. Schroeder, P. D. Angelo, S. E. Watkins, K. Song, T. D. Anthopoulos and I. McCulloch, *Chem. Commun.*, 2012, **48**, 5832.
9 (*a*) G. Y. Chen, C. M. Chiang, D. Kekuda, S. C. Lan, C. W. Chu and K. H. Wei, *J. Polym. Sci., Part A: Polym. Chem.*, 2010, **48**, 1669; (*b*) S. Qu and H. Tian, *Chem. Commun.*, 2012, **48**, 3039; (*c*) B. Walker, A. B. Tamayo, X. Dung, P. Zalar, J. H. Seo, A. Garcia, M. Tantiwiwat and T. Q. Nguyen, *Adv. Funct. Mater.*, 2009, **19**, 306; (*d*) J. S. Ha, K. H. Kim and D. H. Choi, *J. Am. Chem. Soc.*, 2011, **133**, 10364; (*e*) L. Huo, J. Hou, H. Y. Chen, S. Zhang, Y. Jiang, T. L. Chen and Y. Yang, *Macromolecules*, 2009, **42**, 6564; (*f*) J. C. Bijleveld, A. Zoombelt, S. G. J. Mathijssen, M. M. Wienk, M. Turbiez, D. M. Leeuw and R. A. J. Janssen, *J. Am. Chem. Soc.*, 2009, **131**, 16616; (*g*) J. C. Bijleveld, V. S. Gevaerts, D. D. Nuzzo, M. Turbiez, S. G. J. Mathijssen, D. M. Leeuw, M. M. Wienk and R. A. J. Janssen, *Adv. Mater.*, 2010, **22**, E242; (*h*) C. H. Woo, P. M. Beaujuge, T. W. Holcombe, O. P. Lee and J. M. J. Fréchet, *J. Am. Chem. Soc.*, 2010, **132**, 15547; (*i*) J. C. Bijleveld, R. A. M. Verstrijden, M. M. Wienk and R. A. J. Janssen, *J. Mater. Chem.*, 2011, **21**, 9224; (*j*) L. Dou, J. Gao, E. Richard, J. You, C. C. Chen, K. C. Cha, Y. He, G. Li and Y. Yang, *J. Am. Chem. Soc.*, 2012, **134**, 10071.
10 (*a*) J. M. Jiang, P. A. Yang, H. C. Chen and K. H. Wei, *Chem. Commun.*, 2011, **47**, 8877; (*b*) J. C. Bijleveld, M. Shahid, J. Gilot, M. M. Wienk and R. A. J. Janssen, *Adv. Funct. Mater.*, 2009, **19**, 3262.
11 (*a*) L. J. Huo, S. Q. Zhang, X. Guo, F. Xu, Y. F. Li and J. H. Hou, *Angew. Chem., Int. Ed.*, 2011, **50**, 9697; (*b*) Y. Huang, X. Guo, F. Liu, L. J. Hou, Y. N. Chen, T. P. Russell, C. C. Han, Y. F. Li and J. H. Hou, *Adv. Mater.*, 2012, **24**, 3383; (*c*) B. Liu, X. Chen, Y. He, Y. F. Li, X. Xu, L. Xiao, L. Li and Y. P. Zou, *J. Mater. Chem. A*, 2013, **1**, 570.
12 (*a*) C. Melzer, E. J. Koop, V. D. Mihailetchi and P. W. Blom, *Adv. Funct. Mater.*, 2004, **14**, 865; (*b*) Y. T. Chang, S. L. Hsu, M. H. Su and K. H. Wei, *Adv. Mater.*, 2009, **21**, 2093.
13 (*a*) E. Zhou, Q. Wei, S. Yamakawa, Y. Zhang, K. Tajima, C. Yang and K. Hashimoto, *Macromolecules*, 2010, **43**, 821; (*b*) J. Pommerehne, H. Vestweber, W. Guss, R. F. Mahrt, H. Bassler, M. Porsch and J. Daub, *Adv. Mater.*, 1995, **7**, 551; (*c*) Y. Liang, D. Feng, Y. Wu, S. T. Tsai, G. Li, C. Ray and L. P. Yu, *J. Am. Chem. Soc.*, 2009, **131**, 7792.
14 (*a*) Y. Zou, D. Gendron, R. Neagu and M. Leclerc, *Macromolecules*, 2009, **42**, 6361; (*b*) L. Huo, J. Hou, H. Y. Chen, S. Zhang, Y. Jiang, T. L. Chen and Y. Yang, *Macromolecules*, 2009, **42**, 6564; (*c*) Y. Zhu, R. D. Champion and S. A. Jenekhe, *Macromolecules*, 2006, **39**, 8712.
15 (*a*) J. L. Bredas, D. Beljonne, V. Coropceanu and J. Cornil, *Chem. Rev.*, 2004, **104**, 4971; (*b*) B. C. Thompson and J. M. Frechet, *Angew. Chem., Int. Ed.*, 2008, **47**, 58; (*c*) M. C. Scharber, D. Muhlbacher, M. Koppe, P. Denk, C. Waldauf, A. J. Heeger and C. J. Brabec, *Adv. Mater.*, 2006, **18**, 789.
16 P. T. Wu, F. S. Kim, R. D. Champion and S. A. Jenekhe, *Macromolecules*, 2008, **41**, 7021.
17 C. J. Brabec, A. Cravino, D. Meissner, N. S. Sariciftci, T. Fromherz, M. T. Rispens, L. Sanchez and J. C. Hummelen, *Adv. Funct. Mater.*, 2001, **11**, 374.
18 M. Y. Chiu, U. S. Jeng, M. S. Su and K. H. Wei, *Macromolecules*, 2010, **43**, 428.

